SUPPLEMENTAL MATERIALS

Supplemental Figures S1-S5

SUPPLEMENTAL FIGURE LEGENDS

Supplemental Figure S1: Purification of testicular spermatozoa and effects of sperm washing on RNA recovery. Related to Figure 1.

A) DIC images of purified testicular germ cells: spermatocytes, early and late round spermatids (scale bar = 18 μm), and mature testicular spermatozoa (scale bar = 6 μm).

B) Effects of sperm washing on major RNA subclasses. Small RNAs were mapped successively to rRNAs, tRNAs, microRNAs, piRNAs (combining reads mapping to repeatmasker with those mapping to unique piRNA transcripts (Li et al., 2013)), and RefSeq. MicroRNA removal by even the lowest-stringency detergent washing protocol presumably reflects the removal of excess adherent epididymosomes or ribonucleoprotein complexes from the surface of sperm – indeed, the specific microRNAs lost include species that are particularly abundant in partially-purified epididymosome preparations relative to sperm (Sharma et al., 2016). Although we and others have shown that epididymosomes deliver their RNA contents to sperm ((Reilly et al., 2016; Sharma et al., 2016) and see below), “epididymosome” preparations represent a heterogeneous mixture of species, including both exosomes and microvesicles, and deriving from various molecularly-distinct regions throughout the epididymis (Sullivan and Saez, 2013). We therefore speculate that RNAs relatively enriched in epididymosomes, and lost upon detergent washing of sperm, are present in a subpopulation of vesicles or ribonucleoprotein complexes that fuse relatively inefficiently with sperm, or are present in the epididymal lumen at levels in excess of those which saturate the relevant receptor on sperm.

C) Heatmap showing individual RNA species exhibiting significant (t test, $p_{adj} < 0.05$) differences between different wash conditions.

Supplemental Figure S2: RNA extraction and enzyme manipulations. Related to Figure 1.

Pie charts for overall RNA composition for untreated or PNK-treated small RNA libraries isolated from testis, cauda epididymis, caput sperm, or cauda sperm. A) shows mapping data including rRNA-mapping reads, which are dramatically enriched following PNK treatment in all populations examined. It will obviously be of interest to determine

whether any of the rRNA fragments uncovered by PNK treatment exhibit functions akin to those being uncovered for tRNA fragments, or whether they are simply nonfunctional degradation intermediates. B) shows the same data after excluding rRNA-mapping reads.

Supplemental Figure S3: Caput sperm have comparable levels of small RNAs to testicular spermatozoa. Related to Figures 1-3.

Data for three replicate small RNA cloning experiments in which two spike-in oligonucleotides were added to testicular spermatozoa or caput epididymal sperm prior to RNA extraction and small RNA-Seq. Although the cloning efficiencies for the oligos differed, both oligos exhibited the same relative change in abundance between the two samples. Data show individual ratios for testicular sperm RNA levels vs. caput sperm, with dots showing individual values (data for the two oligos are shown as different color dots) and mean and standard deviation shown as lines. Note that these samples were cloned without PNK treatment – in two preliminary replicates carried out with PNK treatment, we were unable to detect the spike-ins in the caput sperm sample, suggesting that overall small RNA levels are in fact far higher in caput sperm than testicular sperm (consistent with the gains of tRFs and rRNA fragments we document in PNK-treated cauda sperm RNA – **Figures 1C-E** and **Supplemental Figure S2**). We nonetheless present these data as even with readily-cloned RNAs it is clear that gain of tRFs in the epididymis is not simply a function of massive global destruction of RNAs from testicular sperm resulting in rare pre-existing tRFs being revealed.

Supplemental Figure S4: Validation of TU-tracer expression in caput epididymis. Related to Figures 5-6.

A) Full Western blots corresponding to the cropped panels in **Figure 5B**. Relevant protein size markers are annotated for each image.

B) Full Western blots corresponding to the cropped panels in **Figure 6B**. Relevant protein size markers are annotated at the left of each image.

C) Dot blots for RNA isolated from TU tracer animals expressing *Defb41-Cre* mice, either injected with 4-TU or vehicle alone. Only upon 4-TU injection, RNAs are specifically labeled in caput epididymis and not in control tissues (testis and cauda epididymis)

D) Cumulative distribution plots for all individual microRNAs (>1000 reads) in the testis and cauda sperm dataset, as indicated. X axis shows the $\log_2$ fold change (4-TU-

injected/uninjected) for U->C mutation rates. In both replicates, the right shift in the curve for sperm indicates significant (KS p = 0.0003 for top panel, 0.0027 for bottom panel) enrichment of 4-TU-induced mutations, relative to the testis control.

Supplemental Figure S5: 3’ tRFs are abundant in the epididymis. Related to Figures 1-6.

Northern blots for the 3’ ends of tRNA-Val-CAC and tRNA-Gly-GCC (A), and of both 5’ and 3’ ends for tRNA-Val-CAC (B), in the indicated tissues – intact testes, caput epididymis, or cauda epididymis, or the tissue culture line PC1. In both cases, tRNAs are completely intact in the testis, with robust tRNA cleavage confined to the epididymis, consistent with prior results reported for 5’ tRNA fragments (Sharma et al., 2016). Comparison of intact tRNA bands with the Val-CAC 5’ and 3’ cleavage products (B) suggests roughly similar levels of 5’ and 3’ tRFs are present following tRNA cleavage, demonstrating that the scarce 3’ tRFs present in deep sequencing datasets result from an inability to clone these RNAs rather than an absence of 3’ tRFs.

Figure S1

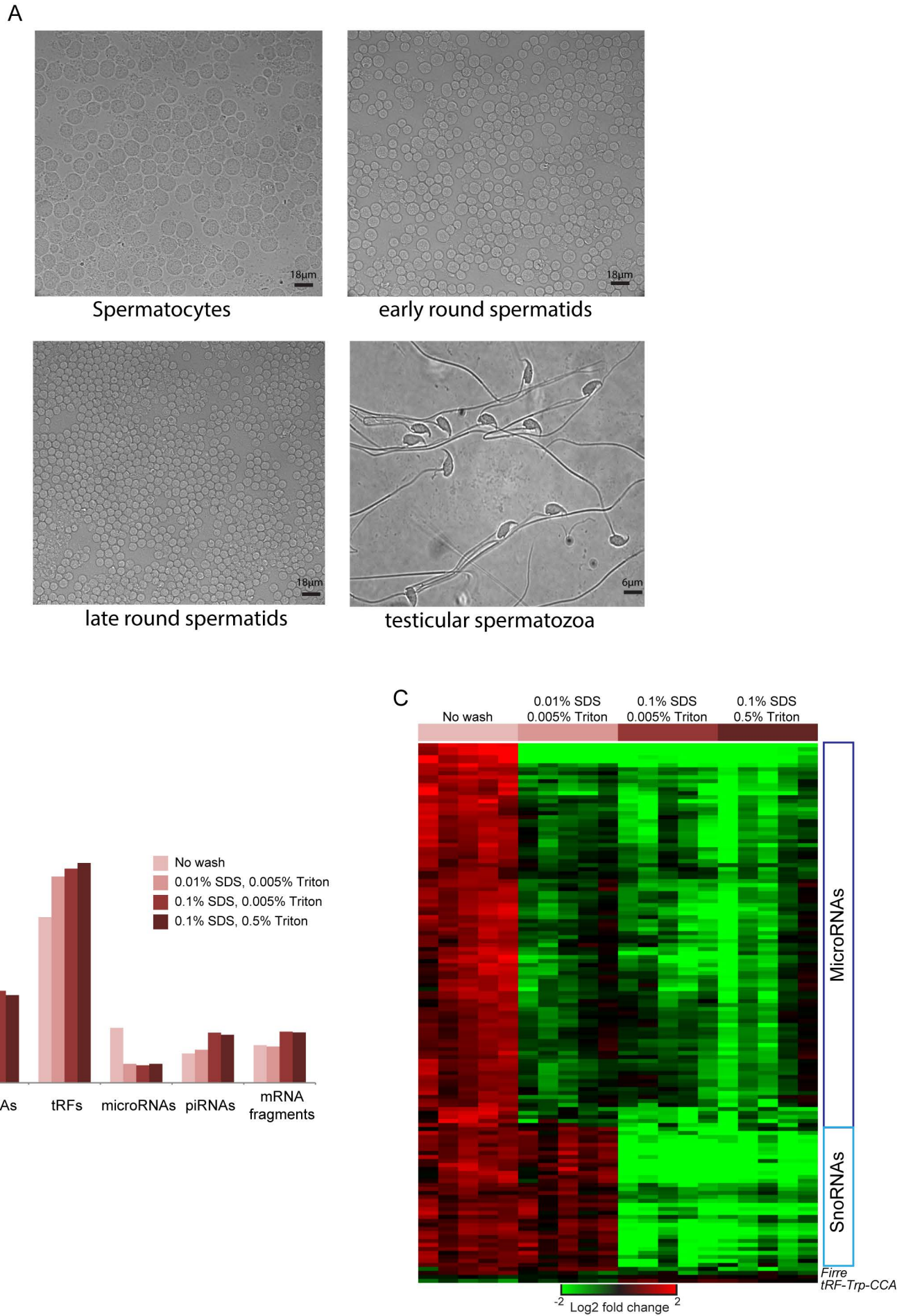
A
18µm
Spermatocytes
18µm
early round spermatids
18µm
late round spermatids
6µm
testicular spermatozoa
B
% of all genome-mapping reads
60
50
40
30
20
10
0
No wash
0.01% SDS, 0.005% Triton
0.1% SDS, 0.005% Triton
0.1% SDS, 0.5% Triton
rRNAs
tRFs
microRNAs
piRNAs
mRNA fragments
C
No wash
0.01% SDS 0.005% Triton
0.1% SDS 0.005% Triton
0.1% SDS 0.5% Triton
MicroRNAs
SnoRNAs
Firre
tRF-Trp-CCA
-2
Log2 fold change
2

Figure S2

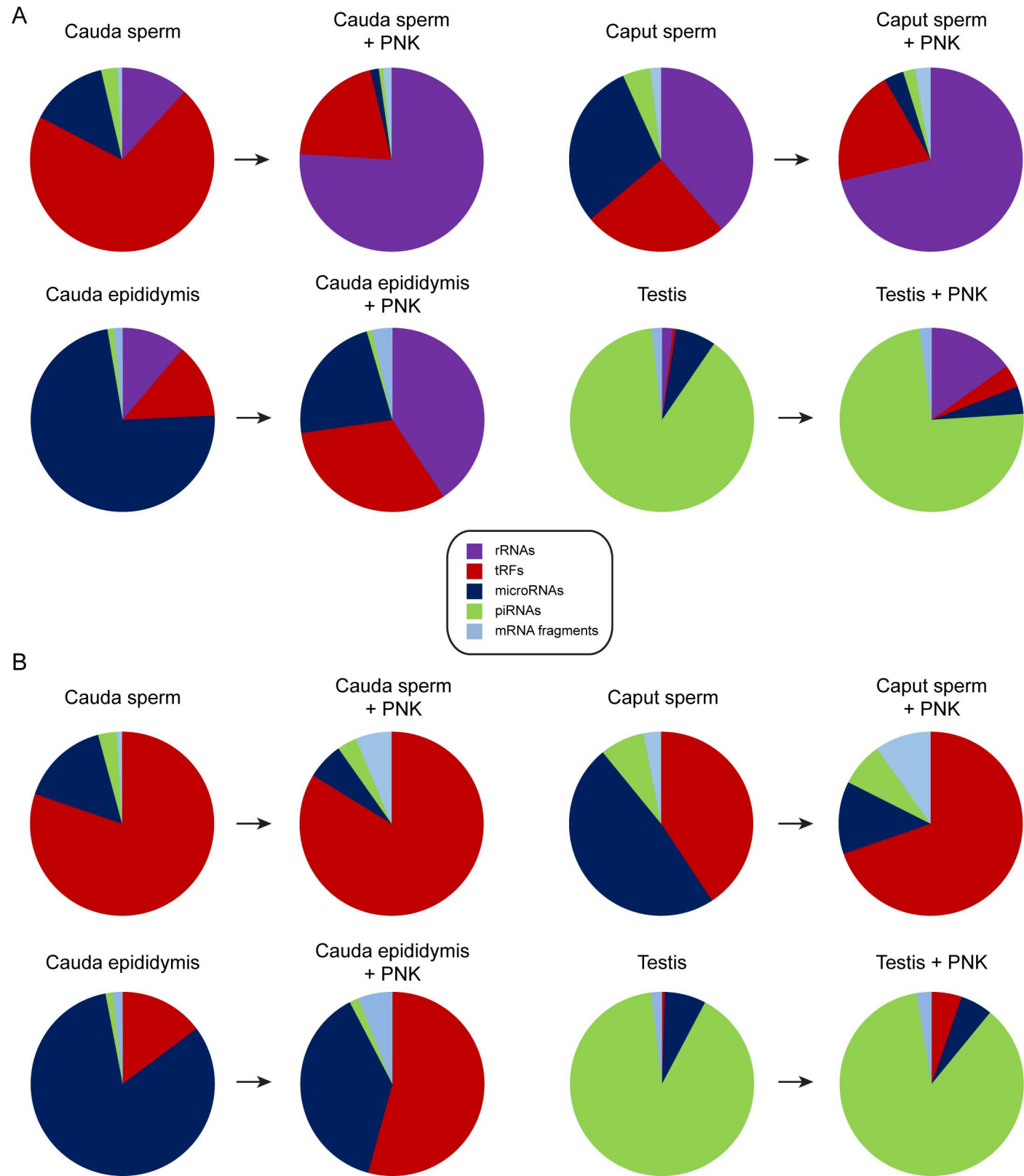
A
Cauda sperm
Cauda sperm + PNK
Caput sperm
Caput sperm + PNK
Cauda epididymis
Cauda epididymis + PNK
Testis
Testis + PNK
rRNAs
tRFs
microRNAs
piRNAs
mRNA fragments
B
Cauda sperm
Cauda sperm + PNK
Caput sperm
Caput sperm + PNK
Cauda epididymis
Cauda epididymis + PNK
Testis
Testis + PNK

Figure S3

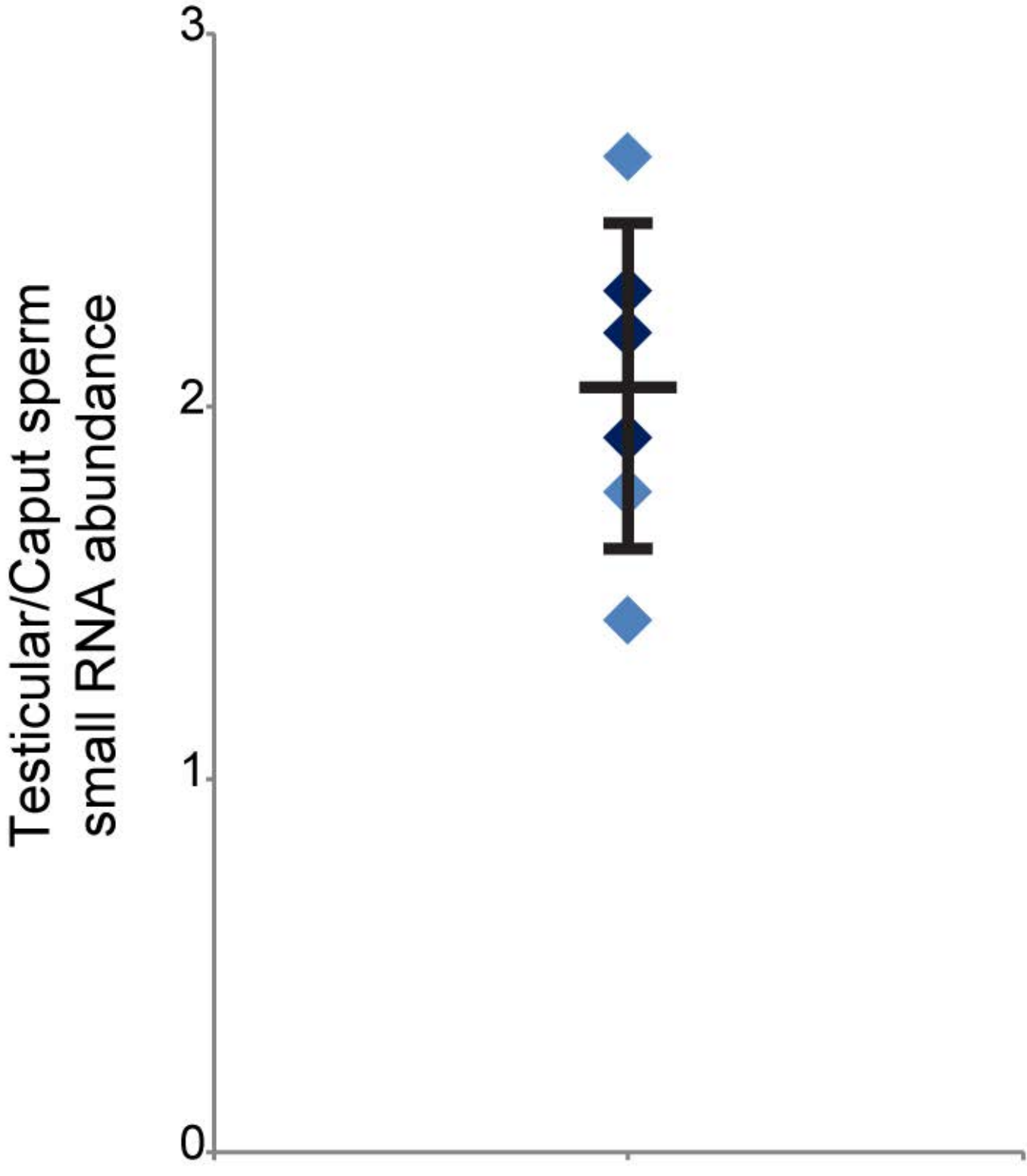

Figure S4

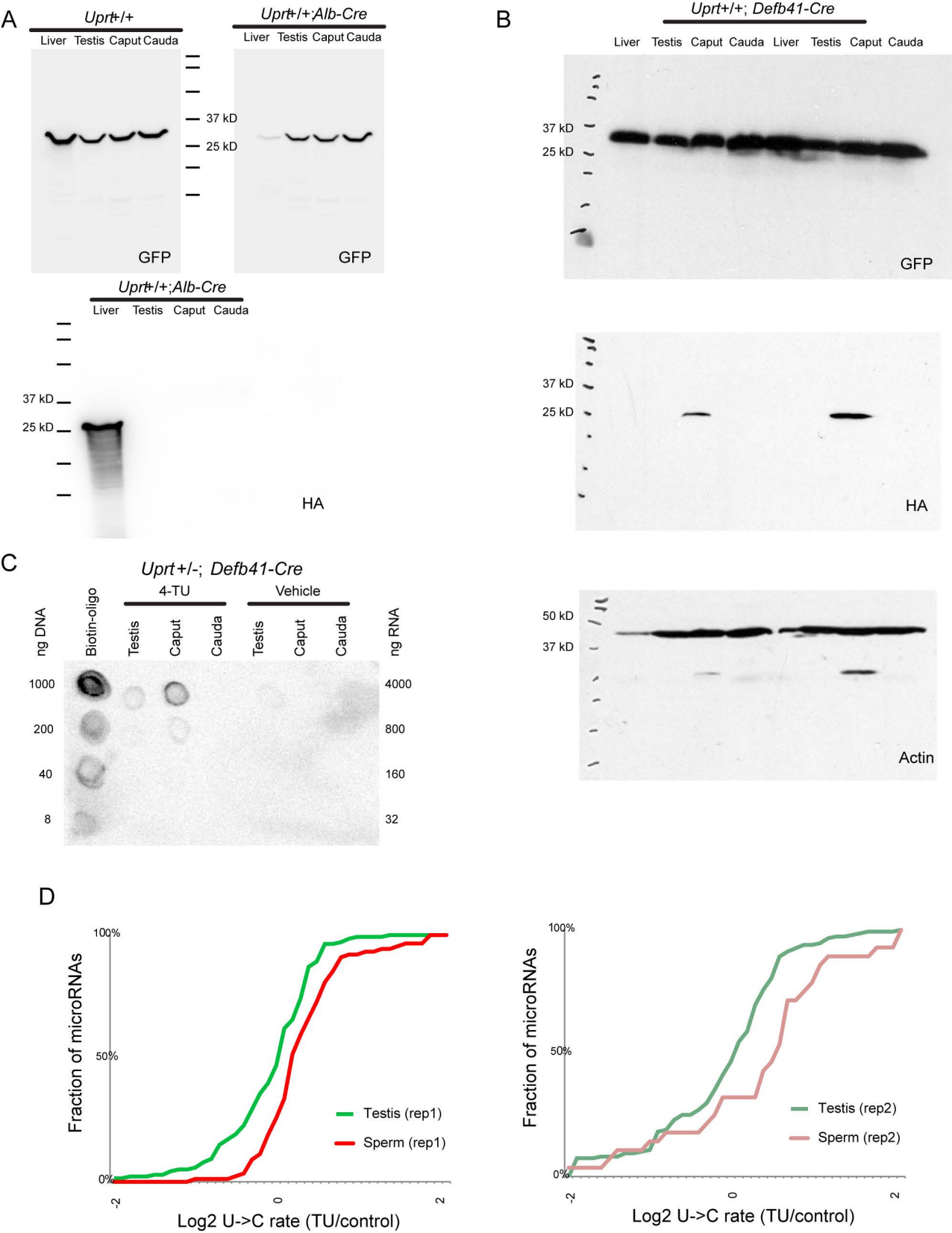
A
Uprt+/+
Liver Testis Caput Cauda
Uprt+/+;Alb-Cre
Liver Testis Caput Cauda
37 kD
25 kD
GFP
GFP
Uprt+/+;Alb-Cre
Liver Testis Caput Cauda
37 kD
25 kD
HA
B
Uprt+/+; Defb41-Cre
Liver Testis Caput Cauda Liver Testis Caput Cauda
37 kD
25 kD
GFP
37 kD
25 kD
HA
50 kD
37 kD
Actin
C
Uprt+/-; Defb41-Cre
4-TU
Vehicle
ng DNA
Biotin-oligo
Testis
Caput
Cauda
Testis
Caput
Cauda
ng RNA
1000
200
40
8
4000
800
160
32
D
Fraction of microRNAs
100%
50%
0%
Testis (rep1)
Sperm (rep1)
-2
0
2
Log2 U->C rate (TU/control)
Fraction of microRNAs
100%
50%
0%
Testis (rep2)
Sperm (rep2)
-2
0
2
Log2 U->C rate (TU/control)

Figure S5

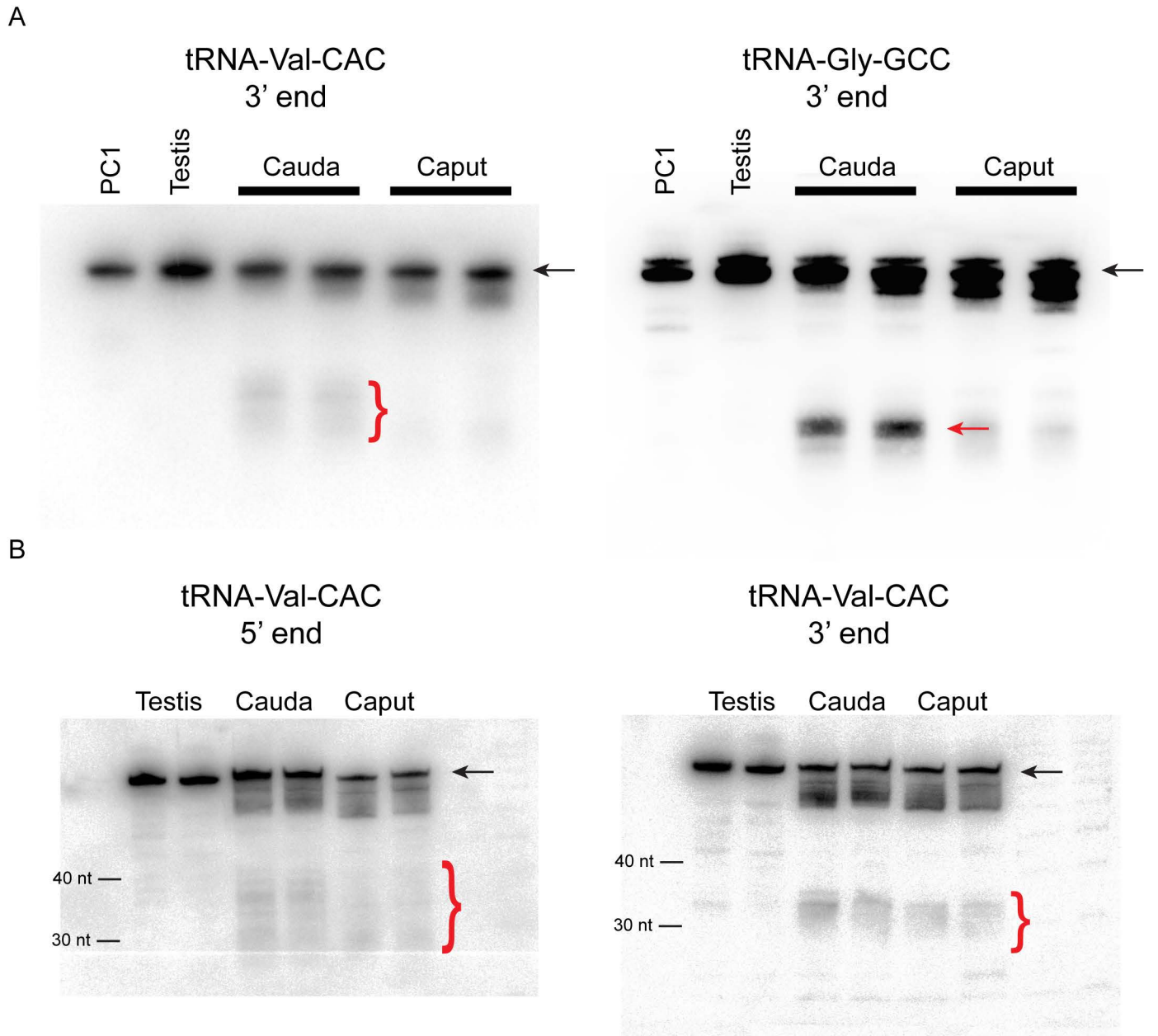
A
tRNA-Val-CAC
3' end
PC1
Testis
Cauda
Caput
tRNA-Gly-GCC
3' end
PC1
Testis
Cauda
Caput
B
tRNA-Val-CAC
5' end
Testis
Cauda
Caput
40 nt
30 nt
tRNA-Val-CAC
3' end
Testis
Cauda
Caput
40 nt
30 nt